

# m-SAAC: Multi-Stage Adaptive Approximation Control to Select Approximate Computing Modes for Vision Applications

Rida Amjad<sup>a</sup>, Rehan Hafiz<sup>1b</sup>, Muhammad U. Ilyas<sup>c,a</sup>, Muhammad Shahzad  
Younis<sup>a</sup>, Muhammad Shafique<sup>d</sup>

<sup>a</sup>*Department of Electrical Engineering  
School of Electrical Engineering and Computer Science (SEECs)  
National University of Sciences and Technology (NUST), Sector H-12, Islamabad,  
Pakistan, 44000*

<sup>b</sup>*Information Technology University (ITU), Lahore, Pakistan*

<sup>c</sup>*Department of Computer and Network Engineering  
College of Computer Science and Engineering*

*University of Jeddah, Jeddah – 23890, Saudi Arabia, 23890*

<sup>d</sup>*The Vienna University of Technology (TU Wien), Austria.*

---

## Abstract

The psycho-visual nature of images and iterative nature of processing algorithms make vision and image processing suitable applications for approximate computing. State-of-the-art research in this area examines application resilience to approximation while assuming a uniform distribution for the information source. In this paper, we demonstrate that data-driven analysis can provide better insight into approximation requirements for image processing applications. Furthermore, this analysis is leveraged to design the multi-stage adaptive approximation control (m-SAAC) methodology that can save compute power by utilizing approximate computing, without compromising on image quality. The results demonstrate the efficacy of the proposed methodology for a variety of test cases.

*Keywords:* Approximate computing, image processing, resilience analysis

---

---

<sup>1</sup>Corresponding author

## 1. Introduction

Moore’s law [1] coupled with Dennard’s scaling rule [2] predicted over three decades of exponential performance increases in the capacity of integrated circuits [3]. Unfortunately, Dennard’s rule no longer applies and, hence, we can improve performance only at the cost of increased power requirements. This divergence between the energy efficiency gains and the transistor integration capacity leads to dark silicon [3]. Approximate computing is being explored to avoid this from happening and be able to sustain both, energy and performance gains, in the long run [4].

Approximate computing involves the relaxation of accuracy in computations resulting in power and area-efficient devices. It is a design paradigm that exploits the resilience to inexactness in computations that is inherent to some applications and uses it to implement more efficient hardware and software. The inherent resilience of these applications can be attributed to several factors, *e.g.*, redundancy present in data, the existence of some computational patterns and the equivalence of a range of similar outputs [5]. However, it must be ensured that approximations do not adversely affect the quality of the results produced by the application [6]. In this regard, some quality thresholds must be maintained, *e.g.*, minimum acceptable accuracy (MAA) and acceptance probability (AP) [7].

Image processing applications are favorable targets for approximate computations since human perception is limited and does not discern errors of small magnitude in image outputs. State-of-the-art approximate circuits [8, 9, 10] show promising results for image processing and vision applications. Furthermore, these circuits typically provide approximation control in order to produce results that can be accurate or provide a particular level of accuracy, while assuming a uniformly distributed input data. This assumption may not hold true for image and video data, specifically for cases where the camera is placed in a static setting, *e.g.*, surveillance cameras, speed cameras, etc. As an example, for a video camera placed in a sports stadium, the green color of the grass shall be pre-dominant. Furthermore, any error in the green region of the image may have a higher psycho-visual impact compared to other regions. To elaborate on this hypothesis, we implemented an approximate low-pass filtering kernel using three configurations of the recently proposed generic GeAr adder[11] (that further correspond to three classical adders: Almost Correct Adder (ACA) [12], Accuracy Configurable Adder (ACA-II) [8] and Gracefully-Degrading Adder (GDA) [13] respectively) and

38 applied it to a set of images.

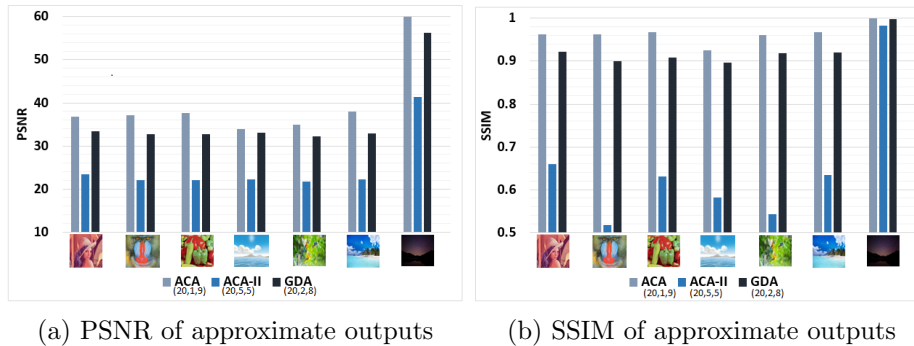


Figure 1: Comparison of PSNR and SSIM of outputs generated by three different approximate adders, *i.e.*, ACA, ACA-II and GDA.

39 Figure 1 compares the output quality in terms of peak signal-to-noise ratio  
 40 (PSNR), a widely used measure of image quality, and multiscale structural  
 41 similarity index measure (SSIM) [14], a psycho-visual measure of error. It  
 42 was observed that for the same adder and kernel, the achieved accuracy  
 43 varied across the images. Particularly for the case of ACA-II configuration,  
 44 it can be observed that the psycho-visual quality, in terms of SSIM, did not  
 45 correlate with the PSNR.

46 *Thus, an input image or a video may have a varying degree of psycho-*  
 47 *visual resilience to a particular approximate circuit depending on content.*  
 48 *Hence, it is desirable to devise analysis methodologies that can aid in better*  
 49 *control of approximation for image processing and computer vision applica-*  
 50 *tions.* To the best of our knowledge, this is the first work that attempts such  
 51 an analysis. In particular, the principal technical contributions of our work  
 52 are the following:

- 53 1. We demonstrate that statistical analysis on images can provide mean-  
 54 ingful insight on the error resilience and hence assess the suitability of  
 55 image data for approximation.
- 56 2. Leveraging from the findings of our analysis, we propose a methodology  
 57 based on some statistical measures (such as kurtosis) that provides a  
 58 data-driven decision to approximate a color channel to a higher or lesser  
 59 degree, depending on its statistical significance in the image.

- 60 3. We further demonstrate that such data-driven control for approxima-  
61 tion provides improved psycho-visual quality. We used several univer-  
62 sally accepted psycho-visual quality metrics to support our findings  
63 [14], [15], [16].
- 64 4. We propose a multi-stage approximation mode selection mechanism  
65 that selects the approximation configurations based on statistical anal-  
66 ysis of the image, thereby providing better approximated output images  
67 than those obtained by assuming a uniform probability distribution of  
68 data.

69 The rest of the paper is organized as follows: Section 2 discusses prior  
70 work done in approximate computing applied to vision applications. Section  
71 3 elaborates on our proposed m-SAAC methodology for data-driven selection  
72 of approximate circuits. Section 4 explains the statistical analysis tools for  
73 image processing applications. Section 5 provides experimental results and  
74 analysis and Section 6 summarizes and concludes the paper.

## 75 2. Literature Review

76 Approximate computing algorithms have been widely applied in image  
77 processing and vision applications, owing to their inherent resilience towards  
78 approximation. Prior work in this area shows approximate circuits applied to  
79 image smoothing [8], image-FFT, inverse-FFT [7], DCT and inverse-DCT [9],  
80 etc. Approximate computing research is not limited to the design of approxi-  
81 mate circuits, but also involves the design of software language extensions to  
82 accommodate approximate instructions and the provision of approximate archi-  
83 tectural support through dedicated approximate units in hardware[17, 18].

84 Approximate language extensions analyze application segments for resi-  
85 lience to approximation and approximate-only soft code slices, *i.e.*, slices  
86 which are amenable to approximations. EnerJ [19] is one such approach that  
87 adds precision type qualifiers to instructions. Hence, at the instruction de-  
88 code stage, the processor will know which instructions will use accurate units  
89 and which are to use approximate computational units.

90 Recently, some approximate computer architectures have been proposed  
91 to facilitate approximate computing. Quality programmable vector processor  
92 is one such abstract model for an approximate computer architecture which  
93 is capable of executing instructions with different quality levels [20].

94 We see approximate computing being applied at the different levels of  
95 design abstractions; namely logical, algorithmic and architectural. However,

96 there is still a dearth of approaches towards disciplined approximate com-  
 97 puting as applied to image processing applications. Research in the area  
 98 of approximate computing applied to images assumes a uniform data distri-  
 99 bution which we believe is not a reasonable assumption. Hence, our work  
 100 targets data-driven approach to predict the resilience of vision applications  
 101 to approximate computing.

### 102 3. Multi-Stage Adaptive Approximation Control

103 A number of image processing and computer vision applications require  
 104 real-time processing of video sequences, *e.g.*, video surveillance systems, high-  
 105 definition television systems, industrial visual inspection systems and vision-  
 106 assisted intelligent robots, to name a few. Due to the computational com-  
 107 plexity involved in real-time video processing, dedicated hardware units are  
 108 typically used for such applications. The approximate computing community  
 109 suggests the use of approximation at different levels of hardware and soft-  
 110 ware. Programming language extensions have been proposed that distinguish  
 111 between accurate and approximate instructions using type qualifiers [19].  
 112 Hardware support is then required for the approximate computations and the  
 113 decision whether to use approximate or accurate computational units is made  
 114 at run-time [20]. We see this run-time decision making as a logic-overhead  
 115 and propose Multi-Stage Adaptive Approximation Control (m-SAAC), an  
 116 offline approximation methodology, that assigns an approximation level for  
 117 a computation depending upon the error resilience of the input data. The  
 118 methodology is illustrated in Figure 2.

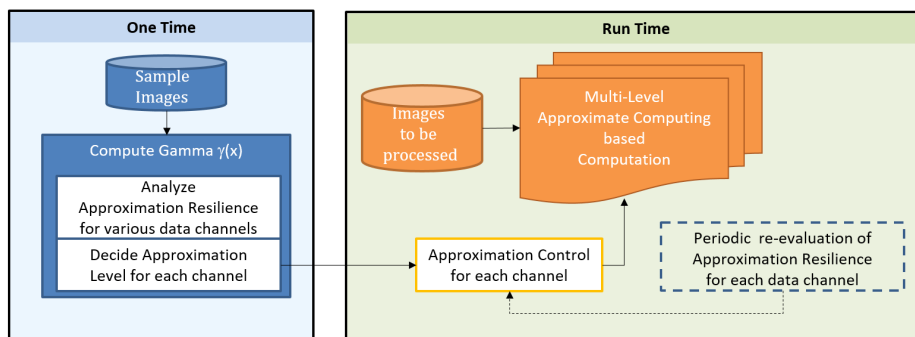


Figure 2: Multi-Stage Adaptive Approximation Control.

119 Computer vision based applications typically involve computations on

120 multiple color channels (Red, Green and Blue). During an initial step our  
121 m-SAAC methodology requires a few samples of application specific RGB  
122 images. These images are analyzed for ranking the error resilience of the  
123 three data channels. Thus, our proposed methodology employs a  $\gamma(x)$  func-  
124 tion, where  $\gamma$  is a statistical function of the image data and  $x$  is the image  
125 itself. Based on the value of  $\gamma(x)$  we rank the RGB channels in order of their  
126 resilience towards approximation. This ranking will differ depending on the  
127 statistical function being considered. Based upon this ranking, m-SAAC shall  
128 control the approximation level for each data channel by selecting the accu-  
129 racy level of an Accuracy Configurable Approximate Circuit. Considering  
130 a streaming application where the ranking may be required to be updated,  
131  $\gamma(x)$  function may be recomputed in a periodic manner to ensure an optimal  
132 quality control for approximate circuit. This ensures that even if significant  
133 visual changes are encountered in the video sequence, our data-driven rank-  
134 ing for error resilience can be re-evaluated. Note that rather than simply  
135 switching the approximation ON or OFF, m-SAAC assigns multiple approx-  
136 imation levels based on the estimated level of resilience. So, for instance, if a  
137 color channel is more resilient to approximation, we can approximate it to a  
138 higher degree. Similarly, for a channel that is less resilient to approximation,  
139 we may not simply turn off the approximation for it rather we may decide to  
140 apply a lower level of approximation. This shall provide a viable compromise  
141 between approximation benefits and accuracy drop.

142 The initial one-time step uses some sample images that are representa-  
143 tive of the data. We believe that if, for instance, we are recording a video  
144 using a static camera, the frames will be similar to the preceding ones since  
145 the background remains steady. Thus, the distribution of RGB values will  
146 remain similar for most of the frames. We verified this hypothesis using the  
147 standard *salesman* video sequence. We computed kurtosis (the motivation  
148 for which will be explained in a later section) for each RGB channel of the  
149 video and provide the plot in Figure 3. It can be observed that relative kur-  
150 tosis wise standing of each color channel is consistent throughout the video  
151 sequence. Thus, for such videos/applications the data may be analyzed of-  
152 fline for estimation of error resilience. Therefore, we analyze the various  
153 statistical measures over some sample images for each RGB channel, select  
154 the most appropriate one and finally decide upon an approximation policy.  
155 This provides us the approximation level for each color channel that is applied  
156 during the run-time multi-level approximate computing based computations.  
157 This data driven decision allows us to achieve approximated outputs that are

158 visually and statistically more acceptable than those achieved through blind  
 159 approximation.

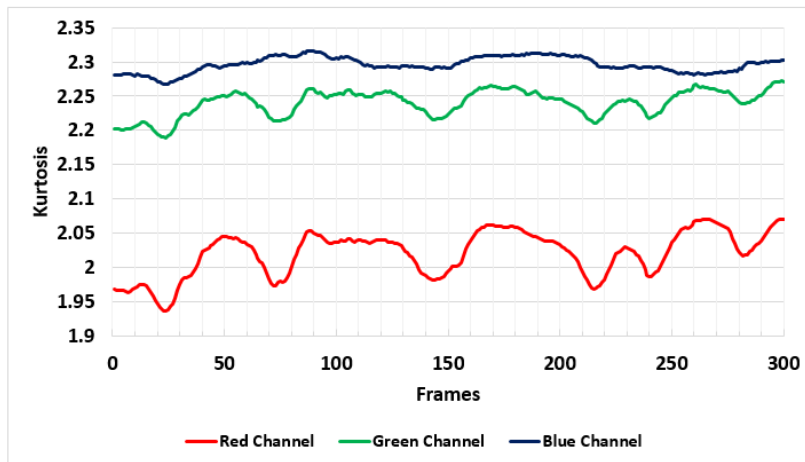


Figure 3: Kurtosis values for RGB channels in the Salesman video sequence.

#### 160 4. Statistical Analysis Functions $\gamma(x)$ for Resilience Analysis

161 In this section we evaluate some image statistics that we believe could  
 162 affect our knowledge of the image content and consequently lead to better  
 163 approximations. These include mean, standard deviation, entropy, median,  
 164 and higher central-moments. As per [21] the mean may not provide a reliable  
 165 representation of the data since it is sensitive to extreme values and any  
 166 outliers in the distribution will push the mean in their direction. The median  
 167 of the data set may not be reliable since it takes the middle value irrespective  
 168 of the dispersion of data present on either sides [21]. The standard deviation  
 169 measures the spread of the data values around the mean and is an indicator  
 170 of data dispersion only[21]. Entropy measures the amount of information in  
 171 the image. An image with little details in structure and contrast will have a  
 172 lower entropy than one with more edges, details and higher contrast. Image  
 173 entropy is calculated using Equation 1 [22] where  $H$  is the image entropy,  $M$   
 174 are the number of gray levels in the image and  $p_k$  is the probability associated  
 175 with gray level  $k$ . Entropy values may be used to assess image quality and,  
 176 hence, make informed decisions about approximating.

$$H = - \sum_{k=0}^{M-1} p_k \log_2 p_k \quad (1)$$

177 Kurtosis measures whether the data in question is peaked or flat, relative  
 178 to a normal distribution. Kurtosis is given by Equation 2 [23].

$$Kurt[X] = E \left[ \left( \frac{X - \bar{x}}{\sigma} \right)^4 \right] = \frac{\mu_4}{\sigma^4}, \quad (2)$$

179 where  $\mu_4$  is the fourth central moment and is defined in Equation 3 [21]

$$\mu_4 = \frac{\sum (x_i - \bar{x})^4}{n} \quad (3)$$

180 and  $\sigma^4$  is given by Equation 4 [21].

$$\sigma^4 = \left( \frac{\sum (x_i - \bar{x})^2}{n} \right)^2 \quad (4)$$

181 Here,  $x_i$  is the pixel value at the  $i^{th}$  location,  $\bar{x}$  is the mean intensity  
 182 value and  $n$  is the number of pixels in the image. To normalize kurtosis, 3  
 183 is subtracted from this result since that is its value for a normal distribu-  
 184 tion. A distribution with a kurtosis value of less than 3 implies that it is  
 185 relatively less outlier-prone than the normal distribution since the tails of its  
 186 distribution are thinner than the tails of a normal distribution[24]. Similarly,  
 187 a distribution with a kurtosis value greater than 3 signifies a distribution  
 188 that is more outlier-prone than the normal distribution since the tails of  
 189 the distribution are fatter than the tails of the normal distribution. Since  
 190 approximation introduces noise (often salt and pepper noise) it can result  
 191 into addition of outliers. Hence, a data channel with a high kurtosis value is  
 192 expected to be more resilient to approximation as compared to the one with  
 193 lower kurtosis value. In the next section we evaluate the suitability of the  
 194 five aforementioned statistical measures for being the  $\gamma(x)$  function.

## 195 5. Results and Discussion

196 In this section we provide the results of our evaluations. We first show  
 197 that selective approximation of color channels, based upon visual analysis,  
 198 can provide results with better psycho-visual quality compared to random

199 selection for approximation. Then we demonstrate that the use of Gamma  
 200 functions can further aid in improved prediction of error resilience for a par-  
 201 ticular color channel. Finally, we show that kurtosis based Gamma function  
 202 provides a reliable error resilience measure and, hence, can be effectively uti-  
 203 lized for our m-SAAC methodology. For our analysis, we specifically consider  
 204 color images since the computational complexity is many-fold. Furthermore,  
 205 for the approximate computing unit we select the GeAr adder model [11]  
 206 due to its wide design space. GeAr’s generic approximate adder model can  
 207 be configured as various state-of-the-art approximate adders, *e.g.*, Almost  
 208 Correct Adder (ACA) [12], Accuracy Configurable Adder (ACA-II) [8] and  
 209 Gracefully-Degrading Adder (GDA) [13]. Furthermore, by varying the Re-  
 210 sultant ( $R$ ) and Prediction ( $P$ ) bits of a GeAr adder, multiple variants with  
 211 varying accuracy levels can be configured. These variants can then be se-  
 212 lected depending upon the error resilience of the input data, as evaluated by  
 213 m-SAAC.

### 214 5.1. Evaluation of Selective Approximation based on Visual Analysis

215 For this evaluation we considered two standard image processing kernels:  
 216 Image blurring and Un-sharp masking. The low-pass filter that we considered  
 217 for image blurring is a non-weighted  $3 \times 3$  filter that assigns the average of  
 218 the values of eight neighbouring pixels and the central pixel to the central  
 219 pixel. The approximate results are generated with three different GeAr adder  
 220 configurations, *i.e.*,  $\text{GeAr}(N,R,P) = (20,1,9)$ ,  $(20,5,5)$  and  $(20,2,8)$ . Here,  $N$   
 221 is the length of the operands to be added while  $R$  and  $P$  are the number  
 222 of resultant and prediction bits. Note that these configurations relate with  
 223 Almost Correct Adder (ACA) [12], Accuracy Configurable Adder (ACA-II)  
 224 [8] and Gracefully-Degrading Adder (GDA) [13].

225 Since, both image blurring and unsharp masking require computations  
 226 to be performed in all the three color channels, we define our selective ap-  
 227 proximation strategy as follows: *We apply approximation to only the color*  
 228 *channel with least visual predominance.* To evaluate this we provide the re-  
 229 sults of low-pass filtering when the approximation is applied to the visually  
 230 most predominant color (*i.e.*, green channel) and visually least predominant  
 231 color (*i.e.*, red channel). The upper and lower rows in Figure 4 show the  
 232 results of low-pass filtering when approximation was applied to green and  
 233 red channels, respectively.

234 Thus, it can be observed that visual predominance based selective ap-  
 235 proximation can result in better results. This is verified by comparing the

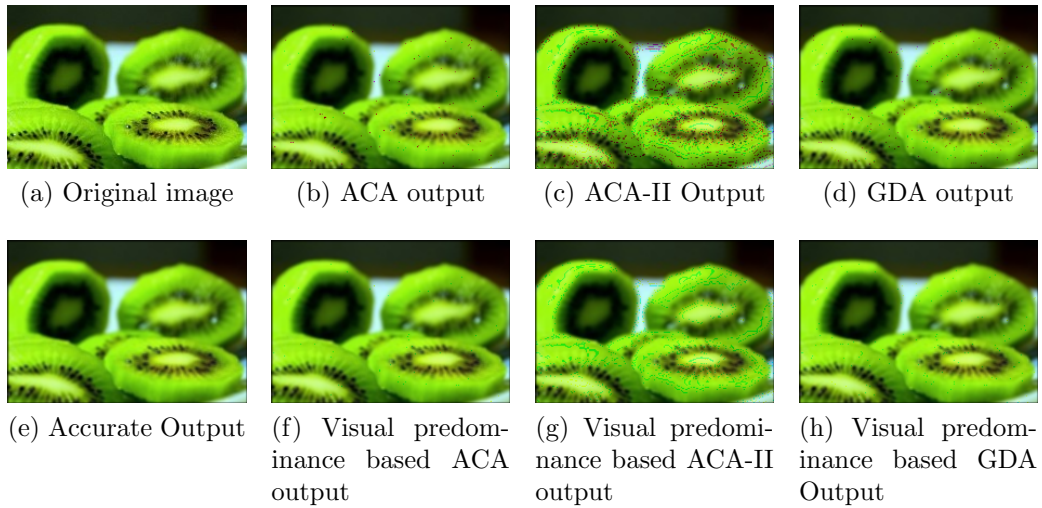


Figure 4: Low-pass filtering of an image accurately and using approximate adders.



Figure 5: Unsharp masking of an image accurately and using approximate adders.

236 results displayed in Figure 4, where the salt and pepper noise is notably lower,  
 237 when red channel is approximated for all three approximate adders. A similar

238 analysis for unsharp masking is shown in Figure 5, where the approximated  
239 results are visually much better for the case (lower row in Figure 5) when  
240 channel with least visual predominance (blue channel) is selected for approx-  
241 imation, compared to when the channel with most visual predominance (red  
242 channel) is selected. *Hence, selective approximation of color channels can be*  
243 *exploited to provide results with better psycho-visual quality.*

## 244 5.2. Evaluation of $\gamma(x)$ functions for Selective Approximation

245 In this section we evaluate the efficacy of utilizing  $\gamma(x)$  function to cor-  
246 rectly predict the approximation resilience of a particular color channel for  
247 selective approximation. For this, we first compared visual predominance  
248 based selection to that of ( $\gamma(x)$ ) based selection where ( $\gamma(x)$ ) was chosen to  
249 be kurtosis function.

250 The following evaluation strategy was performed for selective approxi-  
251 mation. Approximation was switched OFF for the RGB channel that was  
252 predicted least error resilient by Visual Analysis and kurtosis. The remaining  
253 two RGB channels were approximated using the same set of three adders, as  
254 employed in Section 5.1. For the image of Figure 6(a), accurate output of  
255 image blurring is provided in Figure 6(e). Figure 6(b-d) provide the output  
256 when approximation is applied to all color channels. Figure 6(f-h) and (i-k)  
257 provide the outputs when selective approximation is performed based on vi-  
258 sual predominance or kurtosis based  $\gamma(x)$  function, respectively. For visual  
259 predominance based selection, approximation was turned OFF for the blue  
260 channel. For kurtosis based approximation, we turned OFF approximation  
261 for green channel, since it had the lowest kurtosis value among all the RGB  
262 channels and, hence, was least resilient to errors/outliers. Figure 6 shows  
263 that while switching OFF approximation on the blue channel improves the  
264 result compared to where all channels were approximated, the results are still  
265 not optimal. Furthermore, kurtosis based selective approximation is provid-  
266 ing outputs (Figure 6(i-k)) with better visual quality as compared to visual  
267 predominance based. This is particularly noticeable by observing the reduced  
268 noise, specifically in Figure 6(j), compared to Figure 6(g). Thus, the results  
269 further strengthen our hypothesis that statistical measures such as kurto-  
270 sis can be used to effectively minimize errors introduced by approximation  
271 through a data-driven selective approximation.

272 In order to further assess the reliability of kurtosis as a measure for ap-  
273 proximate adder control, we used standard test images used in image process-  
274 ing research as well as natural, everyday images where all colors are present

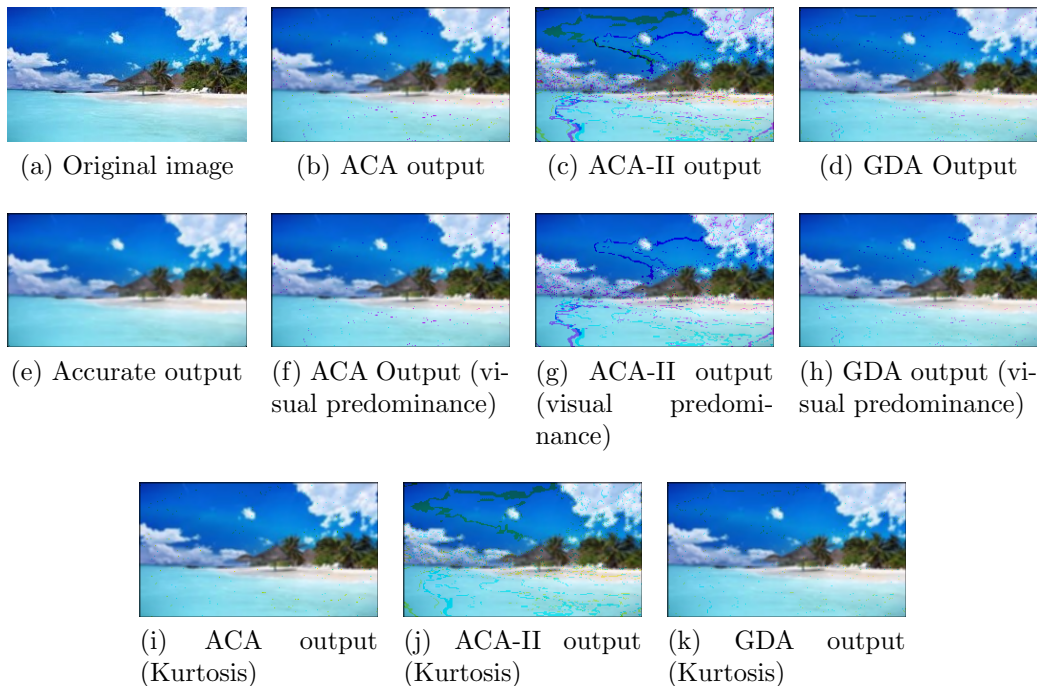
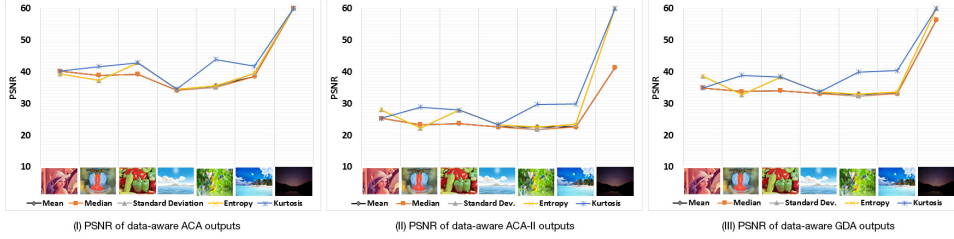
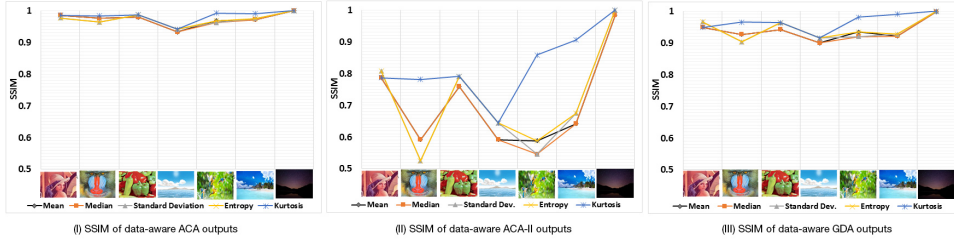


Figure 6: Low-pass filtering of an image using visual predominance and kurtosis as approximation controls.

275 and it is difficult for the human eye to identify the predominant color. We  
 276 compared the set of all possible  $\gamma$  functions in Section 4 and their efficacy in  
 277 predicting the approximation resilience of color channels. As an evaluation  
 278 the approximation was turned OFF for the color channel with least error  
 279 resilience, as predicted by a particular gamma function. Our  $\gamma$  functions  
 280 comprised of mean, median, entropy, standard deviation and kurtosis of the  
 281 image. The higher the value of  $\gamma(x)$  (where  $\gamma$  is the mean, median, entropy  
 282 or standard deviation) the less resilient it is to approximation errors. For  
 283 kurtosis based  $\gamma$ , the lower the value, the less a particular channel is resilient  
 284 to approximation. Thus, for all images under evaluation we applied approxi-  
 285 mation on all color channels, excluding the channel with least error resilience.  
 286 To determine the most efficient  $\gamma$  function, we compared the output quality  
 287 of the results obtained statistically by using PSNR, and psycho-visually, by  
 288 using SSIM. Our results are displayed in Figure 7 and it is evident that kur-  
 289 tosis is the most appropriate measure for the approximation control since it  
 290 gives outputs with higher PSNR and MSSIM for all the tested images. Par-



(a) Statistical Measures comparison using PSNR



(b) Statistical Measures comparison using SSIM

Figure 7: Comparison of statistical measures to judge suitability as approximate computing controls using PSNR and SSIM for the case of image blurring.

291 particularly, for the case illustrated in Figure 7 (a,ii) and (b,ii), kurtosis based  
 292 data-aware ACA-II outputs have an SSIM value that is about 25% higher  
 293 than the SSIM value provided by any other  $\gamma$  function. Since the SSIM index  
 294 is reflective of human vision, kurtosis effectively identifies the color channel  
 295 that is resilient to approximation.

### 296 5.3. Evaluation of Multi-Stage Adaptive Approximation

297 Next, we evaluated our Multi-Stage Adaptive Approximation Scheme (m-  
 298 SAAC) in order to take full advantage of the information derived from the  
 299 image data. For these evaluations, we select kurtosis as our  $\gamma(x)$ , since  
 300 it was demonstrated as the most suitable candidate for the ranking of the  
 301 RGB channels for error resilience in the previous section. For m-SAAC, we  
 302 divided the range of kurtosis values into four ranges or levels, determined  
 303 experimentally. Based on kurtosis value of a particular RGB channel, it is  
 304 assigned one of the levels, as described below.

$$\text{Level1} : \gamma(x) \leq 2.5 \quad (5)$$

305 
$$\text{Level2} : 2.5 < \gamma(x) \leq 3.0 \tag{6}$$

306 
$$\text{Level3} : 3.0 < \gamma(x) \leq 5 \tag{7}$$

307 
$$\text{Level4} : \gamma(x) > 5 \tag{8}$$

308 A channel with a lower kurtosis value is less resilient to approximation  
 309 errors. Thus, our m-SAAC based adaptive approximation will utilize ap-  
 310 proximate adders with higher accuracy for Level 1. Since, we defined four  
 311 levels of approximation, we populated four variants of approximate adders  
 312 utilizing the GeAr adder model. These adder variants are GeAr (N,R,P) =  
 313 (20,1,7), (20,3,5), (20,5,3) and (20,7,1), listed here in the order of increas-  
 314 ing level of approximation. Each of these four variants (numbered 1, 2, 3  
 315 and 4) of approximate adders are associated with their corresponding level  
 316 of accuracy, *i.e.*, Level 1, Level 2, Level 3 and Level 4). As an example, de-  
 317 pending upon the kurtosis value, if red, green and blue channels of an image  
 318 are assigned levels 4, 2 and 4, it means that red, green and blue channels  
 319 shall be processed using the adder variants (20,7,1), (20,3,5) and (20,7,1),  
 320 respectively.

321 For our evaluations, we applied m-SAAC methodology to estimate the ap-  
 322 proximation resilience and hence the associated approximation level for RGB  
 323 channel for our dataset. Figure 8 provides the results for six of these images.  
 324 To have a fair quality comparison, we compare the quality metrics of the  
 325 output image obtained via m-SAAC to that obtained via two other options  
 326 with the same compute cost. For Figure 8(a), m-SAAC selects approxima-  
 327 tion levels (4,4,1) for RGB channels of the Beach image. An approximation  
 328 of (4,4,1) shall represent red, green and blue channel being processed using  
 329 the approximate adder variant 4, 4 and 1, respectively. For a fair comparison,  
 330 we provide the results with the rest of two possible combinations with same  
 331 overall compute cost, *i.e.*, (4,1,4) and (1,4,4). For Figures 8(b-f), m-SAAC  
 332 selects (4,4,1), (4,1,1), (4,4,3), (4,3,3) and (3,4,2), respectively. We used six  
 333 standard psycho-visual and statistical quality measures- namely, multi-scale  
 334 structural similarity index (SSIM), visual information fidelity (VIF), infor-  
 335 mation fidelity criterion(IFC), universal quality index (UQI), visual signal-  
 336 to-noise ratio (VSNR) and peak signal-to-noise ratio (PSNR) to assess the  
 337 quality of the processed output. For all these metrics a higher value repre-  
 338 sents a better quality. It can be observed that m-SAAC is providing con-  
 339 sistently better results on all these quality metrics for a majority of images.

340 It is evident from our analysis that kurtosis effectively captures the approx-  
 341 imate resilience of an image and can be used to rank the color channels in  
 342 order of their resilience to make full use of approximate arithmetic gains  
 343 without compromising on the quality of the approximated output. Thus,  
 344 kurtosis based Gamma function is a reliable measure of error resilience for  
 345 our m-SAAC methodology.

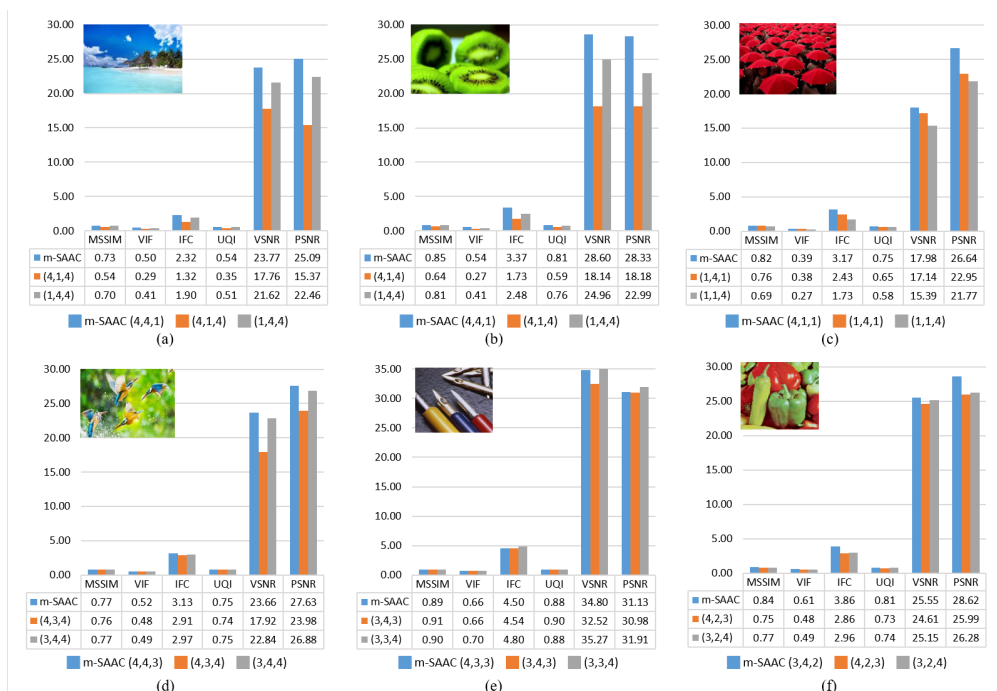


Figure 8: Quality analysis of low-pass filtered results using m-SAAC.

## 346 6. Conclusion

347 This paper justifies the need for data-driven analysis to estimate the er-  
 348 ror resilience of input data. Particularly for image processing and computer  
 349 vision applications, the relative resilience of various color channels can be  
 350 utilized to develop a multi-stage adaptive approximation control for select a  
 351 particular approximation level. The scheme is particularly beneficial for a  
 352 large class of applications characterised by static backgrounds due to station-  
 353 ary nature of camera. Our experimental results demonstrate that kurtosis

354 indeed provides an insight into the error resilience of the input color chan-  
355 nels. Furthermore, the proposed m-SAAC methodology based on disabling  
356 approximation for the color channel with least value of kurtosis provides re-  
357 sults with higher psycho-visual quality as compared to the case where the  
358 decision is arbitrarily made or visually inclined. The paper further extends to  
359 providing an adaptive approximation scheme that estimates RGB channels’  
360 resilience to approximate computing and suggests this scheme as yielding  
361 better quality results than its same compute-cost alternatives.

### 362 **Acknowledgement**

363 This work is supported by HEC (NRPU project) 10150, (AxVision -  
364 Application-Specific Data-Aware, Approximate-Computing for Energy Effi-  
365 cient Image and Vision Processing Applications).”

### 366 **References**

- 367 [1] G. E. Moore, et al., Cramming more components onto integrated cir-  
368 cuits, Proceedings of the IEEE 86 (1998) 82–85.
- 369 [2] R. H. Dennard, V. Rideout, E. Bassous, A. Leblanc, Design of Ion-  
370 implanted MOSFET’s with very small physical dimensions, Solid-State  
371 Circuits, IEEE Journal of 9 (1974) 256–268.
- 372 [3] H. Esmailzadeh, A. Sampson, M. Ringenburg, L. Ceze, D. Grossman,  
373 D. Burger, Addressing dark silicon challenges with disciplined approx-  
374 imate computing, in: Proc. 4th Workshop on Energy-Efficient Design,  
375 pp. 1–2.
- 376 [4] C. M. Kirsch, H. Payer, Incorrect systems: it’s not the problem, it’s  
377 the solution, in: Proceedings of the 49th Annual Design Automation  
378 Conference, ACM, pp. 913–917.
- 379 [5] V. K. Chippa, S. T. Chakradhar, K. Roy, A. Raghunathan, Analysis  
380 and characterization of inherent application resilience for approximate  
381 computing, in: Proceedings of the 50th Annual Design Automation  
382 Conference, ACM, p. 113.
- 383 [6] H. Esmailzadeh, A. Sampson, L. Ceze, D. Burger, Architecture sup-  
384 port for disciplined approximate programming, in: ACM SIGARCH  
385 Computer Architecture News, volume 40, ACM, pp. 301–312.

- 386 [7] N. Zhu, W. L. Goh, W. Zhang, K. S. Yeo, Z. H. Kong, Design of low-  
387 power high-speed truncation-error-tolerant adder and its application in  
388 digital signal processing, *Very Large Scale Integration (VLSI) Systems*,  
389 *IEEE Transactions on* 18 (2010) 1225–1229.
- 390 [8] A. B. Kahng, S. Kang, Accuracy-configurable adder for approximate  
391 arithmetic designs, in: *Proceedings of the 49th Annual Design Automa-  
392 tion Conference*, ACM, pp. 820–825.
- 393 [9] V. Gupta, D. Mohapatra, S. P. Park, A. Raghunathan, K. Roy, IM-  
394 PACT: Imprecise adders for low-power approximate computing, in: *Pro-  
395 ceedings of the 17th IEEE/ACM international symposium on Low-power  
396 electronics and design*, IEEE Press, pp. 409–414.
- 397 [10] J. Han, M. Orshansky, Approximate computing: An emerging paradigm  
398 for energy-efficient design, in: *Test Symposium (ETS), 2013 18th IEEE  
399 European*, IEEE, pp. 1–6.
- 400 [11] M. Shafique, W. Ahmad, R. Hafiz, J. Henkel, A low latency generic  
401 accuracy configurable adder, in: *Proceedings of the 52nd Annual Design  
402 Automation Conference*, ACM, p. 86.
- 403 [12] A. K. Verma, P. Brisk, P. Ienne, Variable latency speculative addition:  
404 A new paradigm for arithmetic circuit design, in: *Proceedings of the  
405 conference on Design, automation and test in Europe*, ACM, pp. 1250–  
406 1255.
- 407 [13] R. Ye, T. Wang, F. Yuan, R. Kumar, Q. Xu, On reconfiguration-oriented  
408 approximate adder design and its application, in: *Proceedings of the  
409 International Conference on Computer-Aided Design*, IEEE Press, pp.  
410 48–54.
- 411 [14] Z. Wang, A. C. Bovik, H. R. Sheikh, E. P. Simoncelli, Image quality as-  
412 sessment: from error visibility to structural similarity, *Image Processing*,  
413 *IEEE Transactions on* 13 (2004) 600–612.
- 414 [15] H. R. Sheikh, A. C. Bovik, Image information and visual quality, *IEEE  
415 Transactions on Image Processing* 15 (2006) 430–444.

- 416 [16] D. M. Chandler, S. S. Hemami, VSNR: A wavelet-based visual signal-  
417 to-noise ratio for natural images, *Image Processing, IEEE Transactions*  
418 *on 16* (2007) 2284–2298.
- 419 [17] M. Shafique, R. Hafiz, S. Rehman, W. El-Harouni, J. Henkel, Cross-layer  
420 approximate computing: From logic to architectures, in: *Proceedings*  
421 *of the 53rd Annual Design Automation Conference, ACM*, p. 99.
- 422 [18] T. Moreau, J. San Miguel, M. Wyse, J. Bornholt, A. Alaghi, L. Ceze,  
423 N. E. Jerger, A. Sampson, A taxonomy of general purpose approximate  
424 computing techniques, *IEEE Embedded Systems Letters* 10 (2018) 2–5.
- 425 [19] A. Sampson, W. Dietl, E. Fortuna, D. Gnanapragasam, L. Ceze,  
426 D. Grossman, EnerJ: Approximate data types for safe and general low-  
427 power computation, in: *ACM SIGPLAN Notices*, volume 46, ACM, pp.  
428 164–174.
- 429 [20] S. Venkataramani, V. K. Chippa, S. T. Chakradhar, K. Roy, A. Raghu-  
430 nathan, Quality programmable vector processors for approximate com-  
431 puting, in: *Proceedings of the 46th Annual IEEE/ACM International*  
432 *Symposium on Microarchitecture, ACM*, pp. 1–12.
- 433 [21] L. Ott, M. Longnecker, R. L. Ott, *An introduction to statistical methods*  
434 *and data analysis*, volume 511, Duxbury Pacific Grove, CA, 2001.
- 435 [22] K. Yanai, K. Barnard, Image region entropy: a measure of visualness  
436 of web images associated with one concept, in: *Proceedings of the 13th*  
437 *annual ACM international conference on Multimedia, ACM*, pp. 419–  
438 422.
- 439 [23] L. T. DeCarlo, On the meaning and use of kurtosis, *Psychological*  
440 *methods* 2 (1997) 292.
- 441 [24] P. Westfall, K. S. Henning, *Understanding advanced statistical methods*,  
442 CRC Press, 2013.